Society For Biomaterials

Cardiac oxidative damage in mice following exposure to nanoparticulate titanium dioxide

Lei Sheng,* Xiaochun Wang,* Xuezi Sang,* Yuguan Ze,* Xiaoyang Zhao, Dong Liu, Suxin Gui, Qingqing Sun, Jie Cheng, Zhe Cheng, Renping Hu, Ling Wang, Fashui Hong

Medical College, Soochow University, Suzhou 215123, China

Received 27 December 2012; accepted 30 January 2013
Published online 2 April 2013 in Wiley Online Library (wileyonlinelibrary.com). DOI: 10.1002/jbm.a.34634

Abstract: Nanoparticulate titanium dioxide (nano-TiO_2) is a widely used powerful nanoparticulate material with high stability, anticorrosion, and photocatalytic property. However, it is possible that during nano-TiO_2 exposure, there may be negative effects on cardiovascular system in intoxicated mice. The present study was therefore undertaken to determine nano-TiO_2-induced oxidative stress and to determine whether nano-TiO_2 intoxication alters the antioxidant system in the mouse heart exposed to 2.5, 5, and 10 mg/kg body weight nano-TiO_2 for 90 consecutive days. The findings showed that long-term exposure to nano-TiO_2 resulted in obvious titanium accumulation in heart, in turn led to sparse cardiac muscle fibers, inflammatory response, cell necrosis, and cardiac biochemical dysfunction. Nano-TiO_2 exposure promoted remarkably reactive oxygen species production such as superoxide radicals, hydrogen peroxide, and increased malondialdehyde, carbonyl and 8-OHdG levels as degradation products of lipid, protein, and DNA peroxidation in heart. Furthermore, nano-TiO_2 exposure attenuated the activities of antioxidative enzymes, such as superoxide dismutase, ascorbate peroxidase, glutathione reductase, glutathione-S-transferase, and levels of antioxidants including ascorbic acid, glutathione, and thiol in heart. Therefore, TiO_2 NPs exposure may impair cardiovascular system in mice, and attention should be aroused on the application of nano-TiO_2 and their potential long-term exposure effects especially on human beings. © 2013 Wiley Periodicals, Inc. J Biomed Mater Res Part A: 101A: 3238–3246, 2013.

Key Words: nanoparticulate titanium dioxide, heart, pathological changes, oxidative stress, antioxidative defense system

How to cite this article: Sheng L, Wang X, Sang X, Ze Y, Zhao X, Liu D, Gui S, Sun Q, Cheng J, Cheng Z, Hu R, Wang L, Hong F. 2013. Cardiac oxidative damage in mice following exposure to nanoparticulate titanium dioxide. J Biomed Mater Res Part A 2013:101A:3238–3246.

INTRODUCTION

The recent development of nanotechnology has provided various innovative nano-materials (NMs). Nano-materials have a large surface area per unit mass, high chemical reactivity, high internal pore volumes, and enhanced cell penetrability. Because of these characteristics, NMs can induce multiple unpredictable effects on human health and the environment. However, despite the growing use of NMs, little is known about their effects in humans and the environment.

Nanoparticulate titanium dioxide (nano-TiO_2) was produced abundantly and used widely in an increasing number of human products including as a white pigment, food colorant, in sunscreens and cosmetic creams, and in environmental decontamination of air, soil, and water because of its high stability, anticorrosion, and photocatalytic property.[1–6] As the interest in the potential benefits of TiO_2 NPs has increased, there is also increasing concern over their potential toxic effects resulting from use or unintentional release into the environment.[7–12]

In recent years, numerous studies have definitely showed that nano-TiO_2 exposure are able to cause the damages in various animal organ types, including lung,[13–15] liver,[16–23] kidney,[24,25] spleen,[26–28] and brain,[29–33] but very little is known about the cardiovascular system (such as heart) damage. Wu *et al*. reported that dermal exposure to nano-TiO_2 in the forms of anatase (4 and 10 nm), rutile (25, 60, and 90 nm) and Degussa P25 (21 nm, anatase/rutile) were suggested to cause significant decreases in the body weight and increases of in the coefficient of liver and spleen in hairless mice, particularly in anatase 10 nm and Degussa P25 treated groups. However, there was no significant

*These authors contributed equally to this work.
Correspondence to: F. Hong; e-mail: Hongfsh_cn@sina.com
Contract grant sponsor: National Natural Science Foundation of China; contract grant numbers: 81273036, 30901218, 8117269
Contract grant sponsor: National Important Project on Scientific Research of China; contract grant number: 2011CB933404
Contract grant sponsor: Priority Academic Program Development of Jiangsu Higher Education Institutions, National New Ideas Foundation of Student of China; contract grant number: 111028534
Contract grant sponsor: "Chun-Tsung scholar" Foundation of Soochow University

change of the heart. They found that nano-TiO_2 could be accumulated in the spleen, heart, and liver after a subchronic dermal exposure, but most of them cannot pass through the blood–brain barrier except Degussa P25. After 8 weeks of exposure to nano-TiO_2, they observed that skin sections from all nano-TiO_2-exposed groups showed excessive keratinization, and other pathological changes such as a thinner dermis and an epidermis with wrinkles, specifically, the anatase 10 nm and P25-exposed groups showed more severe damages. Liver were exhibited as focal necrosis (25 nm, Degussa P25, 60 nm) and liquefaction necrosis (anatase 10 nm). And heart showed only small traces of white blood cells in the anatase 10 nm group, but absence in the other groups. They thought that even though the heart is one of the most important organs, it was not significantly damaged by the accumulated nano-TiO_2 except the anatase 10 nm ones.[29] Particulate matter (PM) exposure is recognized to be one of the most pressing issues in nowadays public health, particularly in relation to the effects on the cardiovascular system. Human exposure to PM has been specifically linked to a number of cardiovascular conditions,[34,35] such as myocardial infarction,[36,37] hypertension,[38,39] atherosclerosis,[40,41] heart rate variability,[42,43] thrombosis,[44,45] and coronary heart disease,[46,47] all occurring because of either direct or indirect mechanisms of action. Therefore, we also hypothesized that long-term exposure to nano-TiO_2 may enter cardiovascular system and result in its damage for human. Thus, the effects of nano-TiO_2 on cardiovascular system need to be elucidated in greater detail.

The oxidative damages of mouse heart caused by exposure to nano-TiO_2 were evaluated in the paper. The results showed that nano-TiO_2 could enter heart and increased reactive oxygen species (ROS) accumulation, decreased activities of the antioxidant enzymes, and antioxidant contents, and promoted oxidation of membrane lipid, protein, and DNA in the heart, in turn led to inflammation, cell necrosis, and sparse cardiac muscle fibers.

MATERIAL AND METHODS

Chemicals, preparation, and characterization

Nanoparticulate anatase TiO_2 was prepared via controlled hydrolysis of titanium tetrabutoxide. Details of the synthesis and characterization of nano-TiO_2 were described in our previous reports.[33,48] X-ray diffraction (XRD) measurements showed that nano-TiO_2 exhibit 101 peak of anatase. The average particle size of powdered nano-TiO_2 which was suspended in 0.5% w/v hydroxypropylmethylcellulose (HPMC) K4M solvent after 24 h incubation ranged from 5 to 6 nm and the surface area of the sample was 174.8 m^2/g. The mean hydrodynamic diameter of nano-TiO_2 in HPMC solvent ranged from 208 to 330 nm (mainly 294 nm), and the zeta potential after 24 h incubation was 9.28 mV, respectively.[33]

Animals and treatment

One hundred fifty CD-1 (ICR) female mice aged 5 weeks (23 $\pm$ 2 g) were purchased from the Animal Center of Soochow University (China). All mice were housed in stainless steel cages in a ventilated animal room. The room temperature of the housing facility was maintained at 24 $\pm$ 2°C with a relative humidity of 60 $\pm$ 10% and a 12-h light/dark cycle. Distilled water and sterilized food were available *ad libitum*. Prior to dosing, the mice were acclimated to the environment for 5 days. All procedures used in animal experiments conformed to the US National Institutes of Health Guide for the Care and Use of Laboratory Animals.[49] Studies were approved by the Soochow University Institutional Animal Care and Use Committee.

A 0.5% HPMC was used as a suspending agent. Nano-TiO_2 powder was dispersed onto the surface of 0.5%, w/v HPMC, and then the suspending solutions containing TiO_2 NPs were treated by ultrasonic for 30 min and mechanically vibrated for 5 min. For the experiment, the mice were randomly divided into four groups ($N = 20$), including a control group (treated with 0.5% w/v HPMC) and three experimental groups [2.5, 5, and 10 mg/kg body weight (BW) nano-TiO_2]. The mice were weighed, and the nano-TiO_2 suspensions were administered to the mice by intragastric administrations every day for 90 days. Any symptom or mortality was observed and recorded carefully everyday during the 90 days. After 90 days, all mice were first weighed, and then sacrificed after being anesthetized using ether. Blood samples were collected from the eye vein by removing the eyeball quickly. Serum was collected by centrifuging blood at 2,500 rpm for 10 min.

Coefficients of heart

After weighing the body and hearts, the coefficients of hearts to body weight were calculated as the ratio of heart (wet weight, mg) to body weight (g).

Titanium content analysis

The hearts were removed from the freezer (−80°C) and thawed. Approximately 0.1 g of the heart was weighed, digested, and analyzed for titanium content. Inductively coupled plasma-mass spectrometry ([ICP-MS] Thermo Elemental X7; Thermo Electron, USA) was used to analyze the titanium concentration in the samples.

Histopathological examination of heart

For pathologic studies, all histopathologic examinations were performed using standard laboratory procedures. The hearts were embedded in paraffin blocks, then sliced (5 μm thickness) and placed onto glass slides. After hematoxylin–eosin (HE) staining, the stained sections were evaluated by a histopathologist unaware of the treatments, using an optical microscope (Nikon U-III Multi-point Sensor System, Japan).

Biochemical assay of myocardium function

In this study, the activity of creatine kinase (CK) in serum was assayed for evaluating myocardium function using a biochemical autoanalyzer (Type 7170; Hitachi, Japan).

Oxidative assay

Superoxide ion (O_2^-) in the heart tissues was measured by monitoring the reduction of XTT in the presence of O_2^-, as

described by Oliveira *et al*.[50] The detection of H_2O_2 in the heart tissues was carried out by the xylenol orange assay.[51]

Lipid peroxidation of hearts was determined as the concentration of malondialdehyde (MDA) generated by the thiobarbituric acid (TBA) reaction as described by Buege and Aust.[52]

Protein oxidation of hearts was investigated according to the method of Fagan *et al*.[53] by determining the carbonyl content. Proteins from heart homogenate were extracted in 50 mM KH_2PO_4 buffer (pH 7.5) containing 10 mM Tris, 2 mM $MgCl_2$, 2 mM EGTA, and 1 mM PMSF. Aliquots of extract were reacted with 10 mM 2,4-dinitrophenylhydrazine dissolved in 2.5*M* HCl for 1 h at room temperature in the dark with vortex every 15 min. Proteins were precipitated with 20% trichloroacetic acid (w/v) and kept on ice for 10 min. After centrifuging at 3,000×*g* for 20 min, protein pellets were washed extensively with ethanol–ethylacetate (1:1) and dissolved in 6*M* guanidine hydrochloride with 20 mM KH_2PO_4 (pH 2.3). The absorbance was recorded at 380 nm after centrifuging at 9,500×*g* for 10 min. The carbonyl content was calculated using the extinction coefficient of 22,000 M^{-1} cm^{-1}.

DNA of hearts was extracted using DNeasy Tissue Mini Kit (Nanjing Jiancheng Bioengineering Institute, Jiangsu, China) as described by the manufacturer. Then, DNA concentration was determined by measuring absorbance at 260 nm using the DNA spectrophotometer (Hitach, Japan). About 38 μL of DNA suspension was incubated at 100°C for 2 min, treated with 3 μL of 250 mM potassium acetate buffer (pH 5.4), 3 μL of 10 mM zinc sulfate, and 2 μL of nuclease P1 (6.25 U/μl; Sigma–Aldrich) at 37°C overnight, and then treated with 6 μL of 0.5*M* Tris–HCl (pH 8.3) and 2 μL of alkaline phosphatase (0.31 U/μl; Sigma–Aldrich), at 37°C for 2 h. Formation of 8-OHdG was determined using the 8-OHdG ELISA kit (Japan Institute for the Control of Aging, Haruoka, Japan). This kit provides a competitive immunoassay for quantitative measurement of the oxidative DNA adduct 8-OHdG. It was carefully performed according to manufacturer's instructions, and using a microplate varishaker-incubator, an automated microplate multi-reagent washer, and a computerized microplate reader.

Antioxidant capacity of hearts

The hearts of mice were homogenized in 1 mL of ice-cold 50 mM sodium phosphate (pH 7.0) that contained 1% polyvinyl polypyrrolidone (PVPP). The homogenate was centrifuged (30,000×*g* for 30 min) and the supernatant was used for assays of activities of SOD, catalase (CAT), ascorbic acid peroxidase (APx), glutathione-S-transferase (GST), and glutathione reductase (GR).

The activity of SOD was assayed by monitoring its ability to inhibit the photochemical reduction of nitroblue tetrazolium (NBT). Each 3 mL reaction mixture contained 50 mM sodium phosphate (pH 7.8), 13 mM methionine, 75 mM NBT, 2 mM riboflavin, 100 mM EDTA, and 200 mL of the enzyme extract. Monitoring the increase in absorbance at 560 nm followed the production of blue formazan.[54]

CAT activity was measured by the decrease in the H_2O_2 concentration for 15 s, reading the absorbance at 240 nm on a UV-3010 absorption spectrophotometer according to Claiborne.[55] The reaction volume was 1 mL and contained 500 mL of sample homogenate and 500 mL of sodium phosphate, buffer 50 mM, pH 7, and 15 mM H_2O_2. The control was assayed without H_2O_2. One unit of enzyme activity was defined as a decrease in absorbance of 0.001 min^{-1} at 240 nm.

APx activity was assayed using the method described by Lundquist and Josefsson.[56] A reaction mixture consisting of 100 mL supernatant, 17 mM H_2O_2 (450 mL), and 25 mM ascorbate (450 mL) was then assayed for 3 min at 290 nm. Activity was measured as disappearance of ascorbate. One unit of enzyme activity was defined as a decrease in absorbance of 0.001 min^{-1} at 290 nm.

GST activity was measured following the method of Habig and Jakoby.[57] The reaction buffer solution contained 100 mM Na-phosphate buffer (pH 6.5), 1 mM 1-chloro-2,4-dinitrobenzene (CDNB) and 1 mM GSH. The reaction was started by the addition of sample solution to the reaction buffer solution. The activity was calculated from the increase in absorbance at 340 nm for 1 min due to CDNB–GSH conjugation when the extinction coefficient was 9.6 $mM^{-1}{\cdot}cm^{-1}$.

GR activity was assayed, as described by Moron *et al*.,[58] with minor modifications. The reaction mixture (1.0 mL) consisted of 100 mM phosphate buffer (pH 7.8), 0.1 mM EDTA, 0.05 mM NADPH, 3.0 mM oxidized glutathione (GSSG), and 50 mL enzyme extract. The reaction was started by the addition of GSSG and the NADPH oxidation rate was monitored at 340 nm for 1.0 min. The activity of GR was calculated as the amount of NADPH oxidized per minute using the molar absorption coefficient of 6.22×10^{-6} for NADPH.

In order to determine reduced glutathione (GSH) and GSSG levels, the hearts were homogenized as described above. GSH and GSSG contents were estimated using the method of Hissin and Hilf.[59] The reaction mixture contained 100 mL of supernatants, 100 mL *o*-phthaldehyde (1 mg/mL), and 1.8 mL phosphate buffer (0.1*M* sodium phosphate, 0.005*M* EDTA, pH 8). Fluorometry was performed using a F-4500 fluorometer (F-4500, Hitachi, Japan) with excitation at 350 nm and emission at 420 nm.

Ascorbic acid (AsA) and dehydroascorbic acid (DHA) determination was determined as described by Jacques-Silva *et al*.[60] Proteins were precipitated in 10 volumes of a cold 4% trichloroacetic acid (TCA) solution. An aliquot of homogenized sample (300 mL), in a final volume of 1 mL of the solution, was incubated at 38°C for 3 h, then 1 mL H_2SO_4 65%(v/v) was added to the medium. The reaction product was determined using color reagent containing 4.5 mg/mL dinitrophenyl hydrazine and $CuSO_4$ (0.075 mg/mL).

Thiol and disulfide contents in the heart were determined by the procedure described by Yee.[61] The hearts were ground and homogenized in 100 mM Tris–HCl buffer (pH 8.6) containing 1 mM EDTA. After centrifuging at 9,500×*g* for 10 min, the supernatant was used for the

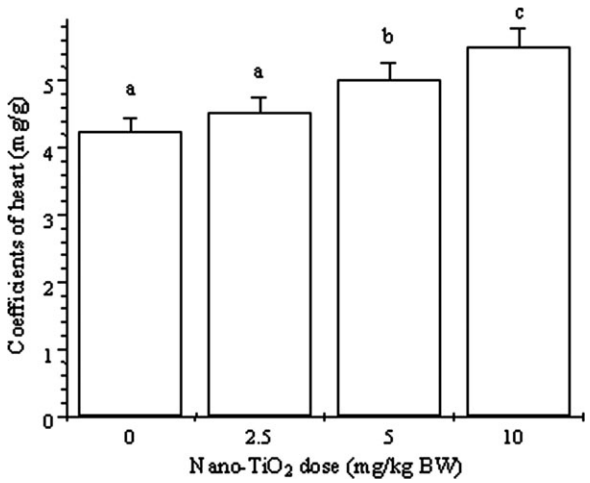

FIGURE 1. Coefficients of heart which were expressed as milligrams (wet weight of tissues)/grams (body weight) of mice caused by an intragastric administration with nano-TiO_2 for 90 consecutive days. Bars marked with different letters means it is significantly different at the 5% confidence level. Values represent means ± SE ($N = 20$).

determination of thiol and disulfide contents. For the determination of thiol content, 100 mL of supernatant was incubated in 880 μL of 8*M* urea Tris–HCl buffer (pH 8.2) with 20 μL of 10 mM 5,5'-dithiobis(2-nitrobenzoic acid) (DTNB) for 30 min at room temperature. Similarly, sample and reagent blanks were prepared for each determination. The absorbance was recorded at 412 nm and thiol content was calculated using the extinction coefficient of 13.6 $mM^{-1}{\cdot}cm^{-1}$. The disulfide bonds were reduced to thiol groups by adding 80 μL of 0.6*M* $NaBH_4$ in 8.0*M* urea into 100 μL of supernatant. Two milliliter *n*-octyl alcohol was added to the mixture to avoid foaming. The mixture was then incubated for 2 h in a water bath at 25°C. The residual $NaBH_4$ was reacted with 20 μL of 2.0*N* HCl and then 778 μL of 8*M* urea Tris–HCl buffer (pH 8.2) was added to it. The mixture was incubated with 20 μL of 10 mM DTNB for 30 min at room temperature. Sample and reagent blanks were prepared for each determination. The absorbance was recorded at 412 nm in order to evaluate the total thiol content, which is the summation of amounts of thiol and (disulfide)/2. The disulfide content was calculated as the half of the difference between the total thiol content and thiol content.

The content of the proteins was determined following the Lowry's method.[62] Each parameter was determined in five animals.

Statistical analysis

Statistical analyses were performed using SPSS 19 software. Data are expressed as the means ± standard error (SE). One-way analysis of variance (ANOVA) was carried out to compare the differences of means among the multi-group data. Dunnett's test was performed when each dataset was compared with the solvent-control data. Statistical significance for all tests was judged at a probability level of 0.05 ($p < 0.05$).

RESULTS

Coefficients of heart and titanium accumulation

The coefficients of heart, titanium accumulation in the mouse heart caused by exposure to nano-TiO_2 for 90 consecutive days are exhibit in Figures 1 and 2, respectively. It can be seen that with increasing nano-TiO_2 dose, the coefficients of heart and titanium contents in the heart were significantly increased ($p < 0.05$ or $p < 0.01$), suggesting that the coefficients of heart may be related to the increases of nano-TiO_2 accumulation and the oxidative injury of heart.

Histopathological evaluation

The histological photomicrographs of the heart sections are shown in Figure 3. Only sparse cardiac muscle fibers of the heart tissue were reflected in the 2.5 mg/kg BW nano-TiO_2-treated group [Fig. 3(b)], compared to the control [Fig. 3(a)]; while severe inflammatory cell infiltration on tunica externa [Fig. 3(c)] and sparse cardiac muscle fibers [Fig. 3(d)] of the heart tissue was showed in the 5 mg/kg nano-TiO_2-treated group, respectively. Particularly, in the 10 mg/kg BW nano-TiO_2-treated group, cell necrosis and sparse cardiac muscle fibers in the heart tissue [Fig. 3(e)] were observed, respectively. The results suggested that with increasing doses of nano-TiO_2 exposure, the pathological changes of heart were more significant.

Biochemical function of myocardium

In Figure 4, the CK activities in the TiO_2 NPs-exposed mice showed obvious increases from the control mice ($p > 0.05$), indicating that nano-TiO_2 exposure may result in myocardium biochemical dysfunction of mice.

ROS accumulation and macromolecule peroxide level*s*

The effects of nano-TiO_2 on the production rate of O_2^- and H_2O_2 in the mouse heart are shown in Figure 5. Compared to the control, ROS contents of all the three stressed groups elevated significantly with increasing nano-TiO_2 doses

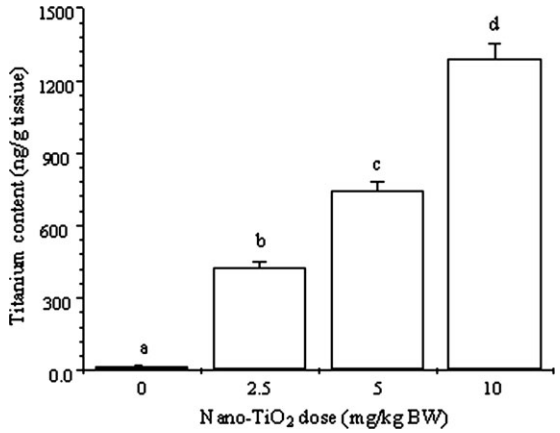

FIGURE 2. Titanium contents which were detected by ICP-MS in the mouse heart caused by an intragastric administration with nano-TiO_2 for 90 consecutive days. Bars marked with different letters means it is significantly different at the 1% confidence level. Values represent means ± SE ($N = 5$).

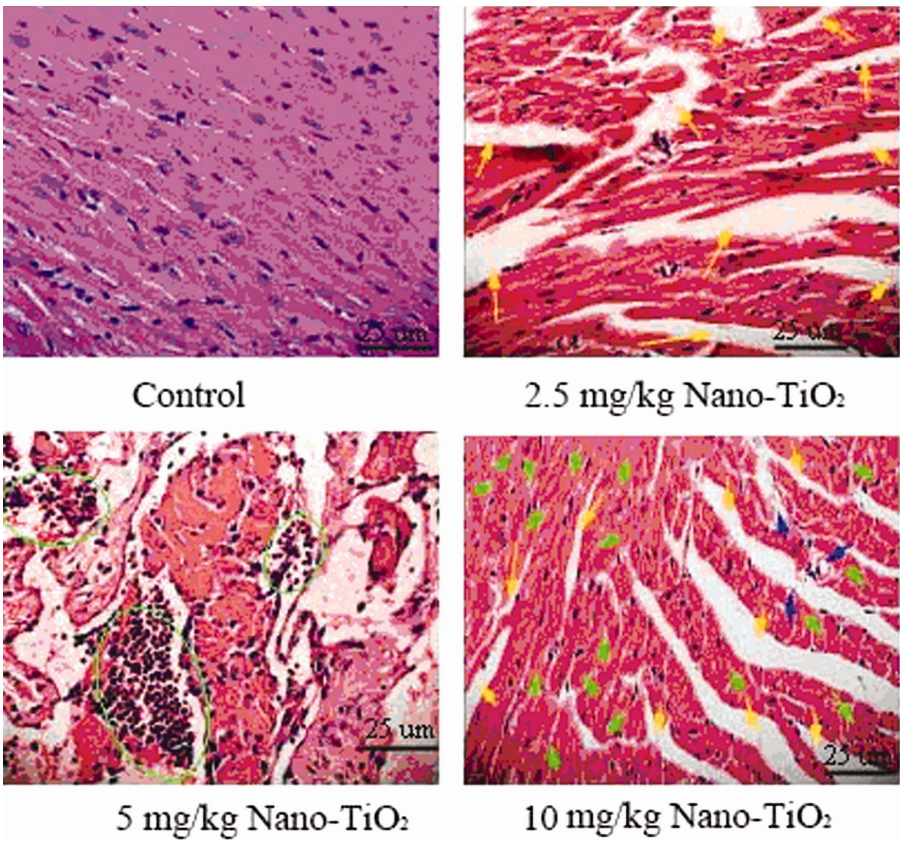

FIGURE 3. Histopathological observation of heart of mice caused by an intragastric administration with nano-TiO_2 for 90 consecutive days. Yellow arrows indicate interspace among the cardiac muscle fibers, blue arrows indicate cell necrosis, green circles show severe inflammatory cell infiltration on tunica externa of the heart tissue. [Color figure can be viewed in the online issue, which is available at wileyonlinelibrary.com.]

($p < 0.05$), suggesting that exposure to nano-TiO_2 caused oxidative stress in the heart.

To demonstrate the effects of nano-TiO_2 on ROS generation, the levels of lipid peroxidation (MDA), protein peroxidation (protein carbonyl), and DNA damage (8-OHdg) in the mouse heart were examined and shown in Figure 6. The marked increases of MDA, carbonyl and 8-OHdG in the nano-TiO_2-exposed hearts were also observed (Fig. 6;

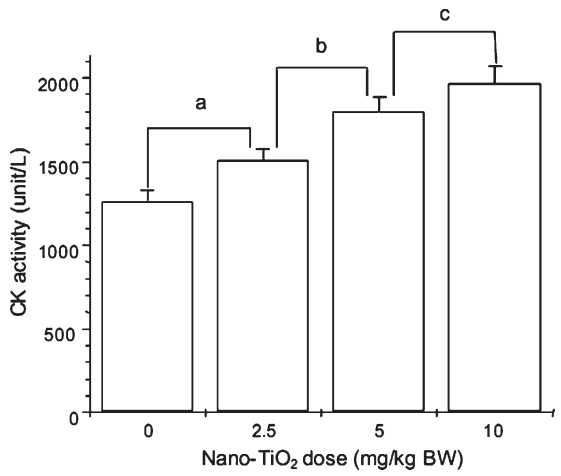

FIGURE 4. Change of biochemical parameter of cardiac function of mice after an intragastric administration with nano-TiO_2 for 90 consecutive days. Bars marked with different letters means it is significantly different at the 5% confidence level. Values represent means ± SE ($N = 5$).

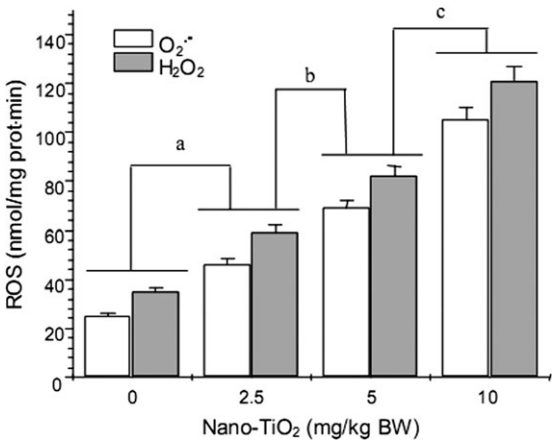

FIGURE 5. ROS accumulation in the mouse heart after an intragastric administration with nano-TiO_2 for 90 consecutive days. Bars marked with different letters means it is significantly different at the 5% confidence level. Values represent means ± SE ($N = 5$).

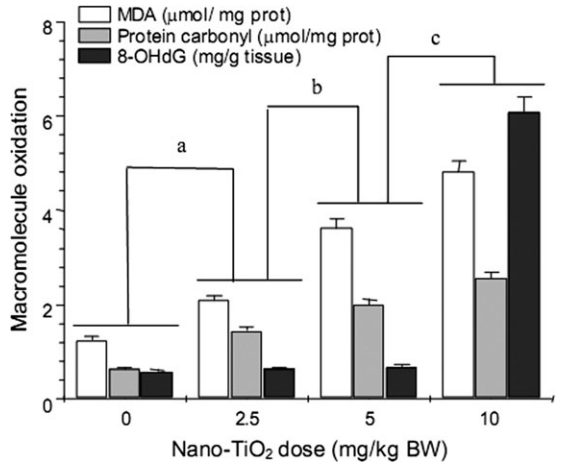

FIGURE 6. Peroxide levels of lipid, protein, and DNA in the mouse heart after an intragastric administration with nano-TiO_2 for 90 consecutive days. Bars marked with different letters means it is significantly different at the 5% confidence level. Values represent means ± SE ($N = 5$).

$p < 0.05$), demonstrating that ROS accumulation led to lipid, protein, and DNA peroxidation in the heart under nano-TiO_2-induced toxicity.

Antioxidant defense

The activities of antioxidative enzymes, including SOD, CAT, APx, GR, and GST, in the heart, were examined (Fig. 7). These enzymes of heart exposed TiO_2 NPs were significantly decreased with elevating nano-TiO_2 doses (Fig. 7; $p < 0.05$). To further explore the effects of nano-TiO_2 stress on antioxidant capacity, the redox states of GSH–GSSG, AsA–DHA, and thiol–disulfide in the hearts were examined and shown in Figure 8. The obvious decreases of GSH, AsA, and thiol in the three nano-TiO_2 stressed groups were also observed ($p < 0.05$). These results suggested that nano-TiO_2 exposure

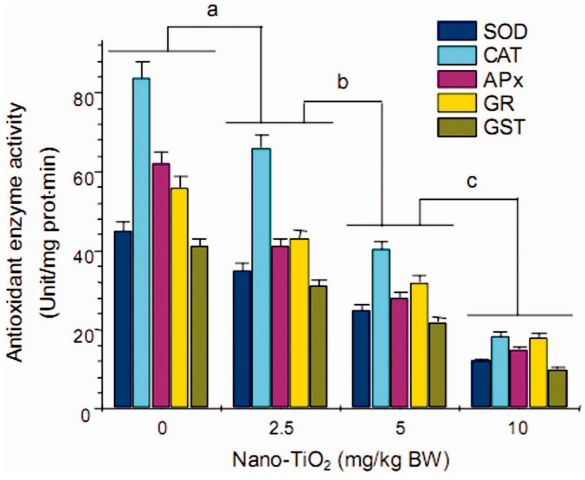

FIGURE 7. Antioxidative enzyme activities in the mouse heart after an intragastric administration with nano-TiO_2 for 90 consecutive days. Bars marked with different letters means it is significantly different at the 5% confidence level. Values represent means ± SE ($N = 5$). [Color figure can be viewed in the online issue, which is available at wileyonlinelibrary.com.]

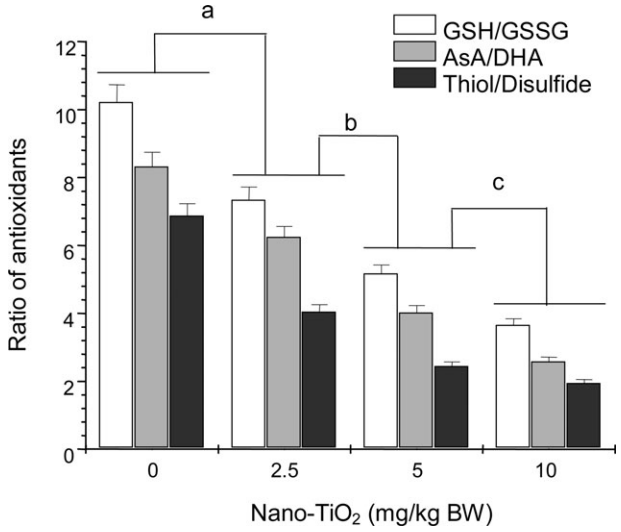

FIGURE 8. Redox states of GSH–GSSG, AsA–DHA, and thiol–disulfide in the mouse heart after an intragastric administration with nano-TiO_2 for 90 consecutive days. Bars marked with different letters means it is significantly different at the 5% confidence level. Values represent means ± SE ($N = 5$).

significantly attenuated the capability of ROS removal in the mouse heart.

DISCUSSION

In this study, toxicological impacts of nano-TiO_2 on heart of mice were evaluated. After the intragastric administration with 2.5, 5, and 10 mg/kg BW of TiO_2 NPs for 90 consecutive days, significant increases of the heart indices (Fig. 1), titanium accumulation (Fig. 2), and sparse cardiac muscle fibers, inflammatory response, and cell necrosis in the heart (Fig. 3) were observed, respectively.

It is well known that CK mainly exists in the heart. Customarily, increased CK level indicates the myocardial lesion.[9] In order to further study the biochemical mechanism of nano-TiO_2, CK activity for the damages of the myocardium biochemical function in the blood was determined. The result shows that long-term TiO_2 NPs exposure caused significant increases of CK activity in the serum, suggesting cardiac biochemical dysfunction of mice. Wang *et al*. and Liu *et al*. reported respectively that exposure to nano-TiO_2 for 2 weeks elevated CK activity in the serum which was associated with myocardium dysfunction of mice, but they did not work in the damaged mechanism.[9,16] In this study, nano-TiO2-induced abnormal pathological change in the heart. In this study, nano-TiO_2-induced abnormal pathological changes and myocardium biochemical dysfunction in the mouse heart may be related to the alterations of antioxidative levels and peroxidation of lipid, protein, and DNA. ROS are ubiquitous in living aerobic organisms. They result either from the cells' metabolism or from the action of exogenous physical sources (e.g., ionizing radiation, UVA) and/or chemical compounds. Oxygen free radicals can induce a variety of damages to lipid, protein, and DNA in cells. Increasing evidences suggested that oxidative stress in the liver,[20,21] kidney,[22] spleen,[24] brain,[30] hippocampus,[33]

lung of mice,[14] and in zebrafish[12] was closely related to nano-TiO_2 exposure. In this article, our data show that long-term exposure to nano-TiO_2 promoted obviously accumulation of ROS such as O_2^-, H_2O_2 in the mouse heart (Fig. 5), which may be linked to the immune cell infiltration (Fig. 3; ROS in the immune cells or produced by the immune cells as they attempt to rid the tissue of particles), and consistent with the marked elevation of lipid, protein, and DNA peroxide levels (Fig. 6), demonstrating that nano-TiO_2 exposure induced severe oxidative stresses in the heart, thus leading to abnormal pathological changes, and biochemical dysfunction of the mouse heart.

In this study, nano-TiO_2-induced ROS production in the mouse heart conducted to oxidative injuries in biological macromolecules, including lipid, protein, and DNA peroxidation. Nano-TiO_2 stress is suggested to lead to extensive lipid peroxidation, which has often been used as a marker of nano-TiO_2-induced oxidative membrane damages of liver,[20,21] kidney,[24] brain,[30] and lung of mice.[14] In this study, we observe that nano-TiO_2 exposure significantly increased MDA content in the hearts (Fig. 6). Protein peroxidation is often generated in organisms, which results in protein structure damage and dysfunction. The carbonyl level of proteins is widely used as an indicator of oxidative protein damage.[63] Elevated carbonyl level has been demonstrated in organisms under various oxidative stresses.[64,65] Our results show an increased carbonyl level in the nano-TiO_2-exposed mouse heart (Fig. 6). Furthermore, over ROS production in cells can not only result in oxidative damages in lipids and proteins, but also conduct to oxidative damage of DNA. Various reagent chemicals are effective in the hydroxylation of the deoxyguanosine residue in DNA. H_2O_2 generation is demonstrated to induce 8-OHdG or 2,6-diamino-4-hydroxy-5-formamidopyrimidine formation,[66,67] while 8-OHdG is by far the most studied oxidative DNA lesion and has caused much attention because of its mutagenic potential.[68] The oxidized guanine residue 8-oxoguanine can pair both in Watson–Crick mode with cytosine and in Hoogsteen mode with adenine. The latter causes G:C→T:A transversion in cells. As suggested in cells of patients with Cockayne syndrome, the deficiency in nucleotide excision repair causes a low level of 8-OHdG repair and a high frequency of G:C→T:A transversion at the site of the lesion. Besides, the transversions are frequent in human cancers and are especially prevalent in the mutational spectrum of the tumor suppressor gene p53. It suggests the significance of 8-OHdG as an endogenous mutagen and its possible role in the process of carcinogenesis.[69] Accordingly, 8-OHdG level in the nano-TiO_2-exposed mouse heart was greatly elevated compared to control (Fig. 6). Therefore, long-term exposure to nano-TiO_2 was demonstrated to cause severe oxidative damages in the mouse heart (Fig. 5).

Impairment of the antioxidant defense system has been suggested to increase protein carbonyl groups in rat exposed to malathion or organophosphate pesticides.[69,70] Elevated levels of MDA, carbonyl, and 8-OHdG in the nano-TiO_2-exposed mouse heart resulted in increased oxidative damages probably due to reduction of the antioxidant capacity in the mouse heart. Consequently, we also evaluated activities of antioxidant enzymes involved in SOD, CAT, APx, GR, and GST, and non-enzymatic antioxidant system such as the redox states of GSH–GSSG, AsA–DHA, and thiol–disulfide in the mouse heart, indicating that nano-TiO_2 exposure greatly suppressed the five enzymes activities (Fig. 7), and attenuated the ratios of GSH/GSSG, AsA/DHA, and thiol/disulfide (Fig. 8). It implies that the production of oxidative stress in cardiac cell is because an unbalance between ROS production and their removal makes macromolecules and membranes damaged, resulting in the cardiac lesion. Our previous studies also demonstrated that nano-TiO_2 exposure resulted in the significant decreases of activities of SOD, CAT, APx, and glutathione peroxidase (GSH-Px), and ratios of GSH/GSSG and AsA/DHA in liver,[20,21] kidney,[24] brain,[30] and hippocampus of mice.[33] In general, organism posses its own active antioxidant defense systems (antioxidative enzymes such as SOD, CAT, APX, GR, and GST, as well as non-enzymatic antioxidants such as AsA, GSH, and thiol) through which production and removal of ROS is kept in balance. SOD converts O_2^- into H_2O_2 and O_2,[54] and CAT and APX reduce H_2O_2 into H_2O and O_2.[71,72] GR plays a key role in oxidative stress by converting GSSG into GSH. Increased GR activity can elevate the GSH/GSSG ratio, which is required for AsA regeneration.[73] As we know, GST can catalyze the detoxification of lipid peroxides and xenobiotics by conjugating them with GSH.[74] Therefore, increased activities of SOD, CAT, APX, GR, and GST can keep a low level of ROS and prevent ROS toxicity and protect cells. AsA can directly interact with and detoxify oxygen free radicals and thus scavenge ROS. GSH is demonstrated to be a key component of the antioxidant network that removes ROS either directly or indirectly by involving in the AsA–GSH cycle.[75,76] The vital role of GSH in the antioxidant defense system is due to its ability to regenerate AsA through DHA reduction that is via the AsA–GSH cycle.[77] GSH also plays an important role in the antioxidant defense system by acting as a substrate or cofactor for some enzymes, and by maintaining the redox state.[74] While thiol is considered to be a highly reactive constituent of protein molecule and it acts as an antioxidant and participates in the detoxification of xenobiotics and toxic substances. Decreased thiol contents under oxidative stress indicate that oxidative stress might induce the oxidation from thiol group to disulfide group, resulting in alteration of the cellular thiol–disulfide redox state.[78] Thiol–disulfide interconversion plays a major role in the regulation of different physiological processes, and depends strongly on the redox state of the thiol pool.[79] In this study, the decreases of antioxidant enzymes activities and antioxidant contents such as AsA, GSH, and thiol in the heart following exposure to nano-TiO_2 were associated with increases in ROS (Fig. 5), and macromolecules peroxide levels (Fig. 6). It suggests that nano-TiO_2 significantly impaired antioxidant defense systems in the mouse heart.

In addition, this study suggests that the oxidative damages in the heart may be similar for lung, liver, kidney, spleen, brain, and so on in animals following various routes, such as inhalation, transdermal absorption, and ingestion, of exposure to nano-TiO_2.

CONCLUSION

In our study, exposed mice to nano-TiO_2 caused an oxidative damage in the heart monitored by an increase in ROS accumulation. The enhancement of MDA, carbonyl, and 8-OHdG levels caused by nano-TiO_2 suggested an oxidative attack that was activated by a decrease of antioxidant defense mechanisms against stress damage measured by analyzing SOD,CAT, APX GR, and GST activities, as well as non-enzymatic antioxidants such as AsA, GSH, and thiol contents. As the antioxidative response of cell was attenuated in the heart following exposure to nano-TiO_2, it caused significant pathological changes and cardiac biochemical dysfunction in the heart. Therefore, our findings will be to benefit the understanding of nano-TiO_2-induced effects on cardiovascular system and arouse the attention of nano-materials application and exposure effects especially on human cardiovascular system for long-term and low-dose exposure.

REFERENCES

1. Ordman H, Berlin M. Titanium. In: Friberg L, Nordberg GF, Vouk VB, editors. Handbook on the Toxicology of Metals, vol. II. Amsterdam: Elsevier; 1986. p595–609.
2. Lomer MCE, Thompson RPH, Powell JJ. Fine and ultrafine particles of the diet: Influence on the mucosal immune response and association with Crohn's disease. Proc Nutr Soc 2002;61:123–130.
3. Gelis C, Girard S, Mavon A, Delverdier M, Paillous N, Vicendo P. Assessment of the skin photoprotective capacities of an organo-mineral broad-spectrum sunblock on two ex vivo skin models. Photodermatol Photoimmunol Photomed 2003;19:242–253.
4. Cho M, Chung H, Choi W, Yoon J. Linear correlation between inactivation of *E. coli* and OH radical concentration in TiO_2 photocatalytic disinfection. Water Res 2004;38:1069–1077.
5. Choi H, Stathatos E, Dionysiou DD. Solgel preparation of mesoporous photocatalytic TiO_2 films and TiO_2/Al_2O_3 composite membranes for environmental applications. Appl Catal B Environ 2006; 63:60–67.
6. Esterkin CR, Negro AC, Alfano OM, Cassano AE. Air pollution remediation in a fixed bed photocatalytic reactor coated with TiO_2. AIChE J 2005;51:2298–2310.
7. Warheit DB, Webb TR, Reed KL, Frerichs S, Sayes CM. Pulmonary toxicity study in rats with three forms of ultrafine-TiO_2 particles: Differential responses related to surface properties. Toxicol 2007; 230:90–104.
8. Wang JJ, Sanderson BJS, Wang H. Cyto- and genotoxicity of ultrafine TiO_2 particles in cultured human lymphoblastoid cells. Mutat Res 2007;628:99–106.
9. Wang JX, Zhou GQ, Chen CY, Yu HW, Wang TC, Ma M. Acute toxicity and biodistribution of different sized titanium dioxide particles in mice after oral administration. Toxicol Lett 2007;168: 176–185.
10. Li JG, Li QN, Xu GY, Li J, Cai XQ, Liu RL. Comparative study on the acute pulmonary toxicity induced by 3 and 20 nm TiO_2 primary particles in mice. Environ Toxic Pharmacol 2007;24:239–244.
11. Wang HH, Wick RL, Xing BS. Toxicity of nanoparticulate and bulk ZnO, Al_2O_3 and TiO_2 to the nematode Caenorhabditis elegans. Environ Pollut 2009;157:1171–1177.
12. Xiong D, Fang T, Yu L, Sima X, Zhu W. Effects of nano-scale TiO_2, ZnO and their bulk counterparts on zebrafish: Acute toxicity, oxidative stress and oxidative damage. Sci Total Environ 2011; 409:1444–1452.
13. Chen HW, Su SF, Chien CT, Lin WH, Yu SL, Chou CC, Chen Jeremy JW, Yang PC. Titanium dioxide nanoparticles induce emphysema-like lung injury in mice. FASEB J 2006;20:1732–1741.
14. Sun QQ, Tan DL, Zhou QP, Liu XR, Cheng Z, Liu G, Zhu M, Sang XZ, Gui SX, Cheng J, Hu RP, Tang M, Hong FS. Oxidative damage of lung and its protective mechanism in mice caused by long-term exposure to titanium dioxide nanoparticles. J Biomed Mater Res A 2012;100:2554–2562.
15. Sun QQ, Tan DL, Ze YG, Sang XZ, Liu XR, Gui SX, Cheng Z, Cheng J, Hu RP, Gao GD, Liu G, Zhu M, Zhao XY, Sheng L, Wang L, Tang M, Fashui Hong FS. Pulmotoxicological effects caused by long-term titanium dioxide nanoparticles exposure in mice. J Hazard Mater 2012;235–236:47–53.
16. Liu HT, Ma LL, Zhao JF, Liu J, Yan JY, Ruan J, Hong FS. Biochemical toxicity of mice caused by nano-anatase TiO_2 particles. Biol Trace Elem Res 2009;129:170–180.
17. Ma LL, Zhao JF, Wang J, Duan YM, Liu J, Li N, Liu HT, Yan JY, Ruan J, Hong FS. The acute liver injury in mice caused by nano-anatase TiO_2. Nanosacle Res Lett 2009;4:1275–1278.
18. Duan YM, Liu J, Ma LL, Li N, Liu HT, Wang J, Zheng L, Liu C, Wang XF, Zhang XG, Yan JY, Wang H, Hong FS. Toxicological characteristics of nanoparticulate anatase titanium dioxide in mice. Biomaterials 2010;31:894–899.
19. Li N, Ma LL, Wang J, Liu J, Duan YM, Liu HT, Zhao XY, Wang SS, Wang H, Hong FS. Interaction between nano-anatase TiO_2 and liver DNA from mice in vivo. Nanoscale Res Lett 2010;5:108–115.
20. Cui YL, Gong XL, Duan YM, Li N, Hu RP, Liu HT, Hong MM, Zhou M, Wang L, Wang H, Hong FS. Hepatocyte apoptosis and its molecular mechanisms in mice caused by titanium dioxide nanoparticles. J Hazard Mater 2010;183:874–880.
21. Liu HT, Ma LL, Liu J, Zhao JF, Yan JY, Hong FS. Toxicity of nano-anatase TiO_2 to mice: Liver injury, oxidative stress. Toxicol Environ Chem 2010;92:175–186.
22. Cui YL, Liu HT, Zhou M, Duan YM, Li N, Gong XL, Hu RP, Hong MM, Hong FS. Signaling pathway of inflammatory responses in the mouse liver caused by TiO_2 nanoparticles. J Biomed Mater Res A 2011;96:221–229.
23. Cui YL, Liu HT, Ze YG, Zhang ZL, Hu YY, Cheng Z, Hu RP, Gao GD, Cheng J, Gui SX, Sang XZ, Sun QQ, Wang L, Tang M, Hong FS. Gene expression in liver injury caused by long-term exposure to titanium dioxide nanoparticles in mice. Toxicol Sci 2012;128: 171–185.
24. Zhao JF, Wang J, Wang SS, Zhao XY, Yan JY, Ruan J, Li N, Duan YM, Wang H, Hong FS. The mechanism of oxidative damage in nephrotoxicity of mice caused by nano-anatase TiO_2. J Exp Nanosci 2010;5:447–462.
25. Gui SX, Zhang ZL, Zheng L, Cui YL, Liu XR, Li N, Sang XZ, Su QQ, Gao GD, Cheng Z, Cheng J, Wang L, Tang M, Hong FS. Molecular mechanism of kidney injury of mice caused by exposure to titanium dioxide nanoparticles. J Hazard Mater 2011;195: 365–370.
26. Li N, Duan YM, Hong MM, Zheng L, Fei M, Zhao XY, Wang Y, Cui YL, Liu HT, Cai J, Gong SJ, Wang H, Hong FS. Spleen injury and apoptotic pathway in mice caused by titanium dioxide nanoparticles. Toxicol Lett 2010;195:161–168.
27. Wang J, Li N, Zheng L, Wang Y, Duan YM, Wang SS, Zhao XY, Cui YL, Zhou M, Cai JW, Gong SJ, Wang H, Hong FS. P38-Nrf-2 signaling pathway of oxidative stress in mice caused by nanoparticulate TiO_2. Biol Trace Elem Res 2011;140:186–197.
28. Sang XZ, Zheng L, Sun QQ, Li N, Cui YL, Hu RP, Gao GD, Cheng Z, Cheng J, Gui SX, Liu HT, Tang M, Hong FS. The chronic spleen injury of mice following long-term exposure to titanium dioxide nanoparticles. J Biomed Mater Res A 2012;100:894–902.
29. Wu JH, Liu W, Xue CB, Zhou SH, Lan FL, Bi L, Xu HB, Yang XL, Zeng FD. Toxicity and penetration of TiO_2 nanoparticles in hairless mice and porcine skin after subchronic dermal exposure. Toxicol Lett 2009;191:1–8.
30. Shin JA, Lee EJ, Seo SM, Kim HS, Kang JL, Park EM. Nanosized titanium dioxide enhanced inflammatory responses in the septic brain of mouse. Neuroscience 2010;165:445–454.
31. Ma LL, Liu J, Li N, Wang J, Duan YM, Yan JY, Liu HT, Wang H, Hong FS. Oxidative stress in the brain of mice caused by translocated nanoparticulate TiO_2 delivered to the abdominal cavity. Biomaterials 2010;31:99–105.
32. Hu RP, Gong XL, Duan YM, Li N, Che Y, Cui YL, Zhou M, Liu C, Wang H, Hong FS. Neurotoxicological effects and the impairment of spatial recognition memory in mice caused by exposure to TiO_2 nanoparticles. Biomaterials 2010;31:8043–8050.
33. Hu RP, Zheng L, Zhang T, Cui YL, Gao GD, Cheng Z, Cheng J, Tang M, Hong FS. Molecular mechanism of hippocampal

apoptosis of mice following exposure to titanium dioxide nanoparticles. J Hazard Mater 2011;191:32–40.
34. Brook RD, Rajagopalan S, Pope CA, Brook JR, Bhatnagar A, Diez-Roux AV, Holguin F, Hong Y, Luepker RV, Mittleman MA, Peters A, Siscovick D, Smith SC, Whitsel L, Kaufman JD. Particulate matter air pollution and cardiovascular disease: an update to the scientific statement from the American Heart Association. Circulation 2010;121:2331–2378.
35. Sun Q, Hong X, Wold LE. Cardiovascular effects of ambient particulate air pollution exposure. Circulation 2010;121:2755–2765.
36. Peters A, Dockery DW, Muller JE, Mittleman MA. Increased particulate air pollution and the triggering of myocardial infarction. Circulation 2001;103:2810–2815.
37. Sullivan J, Sheppard L, Schreuder A, Ishikawa N, Siscovick D, Kaufman J. Relation between short-term fine-particulate matter exposure and onset of myocardial infarction. Epidemiology 2005; 16:41–48.
38. Ibad-Mulli A, Stieber J, Wichmann H, Koenig W, Peters A. Effect of air pollution on blood pressure: A population-based approach. Am J Public Health 2001;91:571–577.
39. Choi JH, Xu QS, Park SY, Kim JH, Hwang SS, Lee KH, Lee HJ, Hong YC. Seasonal variation of effect of air pollution on blood pressure. J Epidemiol Commun Health 2007;61:314–318.
40. Allen RW, Criqui MH, Diez Roux AV, Allison M, Shea S, Detrano R, Sheppard L, Wong ND, Stukovsky KH, Kaufman JD. Fine particulate matter air pollution, proximity to traffic, and aortic atherosclerosis. Epidemiology 2009;20:254–264.
41. Araujo JA, Nel AE. Particulate matter and atherosclerosis: role of particle size, composition and oxidative stress. Part Fibre Toxicol 2009;6:24.
42. Cavallari J, Fang S, Eisen E, Schwartz J, Hauser R, Herrick R. Time course of heart rate variability decline following particulate matter exposures in an occupational cohort. Inhal Toxicol 2008; 20:415–422.
43. Whitsel EA, Quibrera PM, Christ SL, Liao D, Prineas RJ, Anderson GL, Heiss G. Heart rate variability, ambient particulate matter air pollution, and glucose homeostasis: The environmental epidemiology of arrhythmogenesis in the women's health initiative. Am J Epidemiol 2009;169:693–703.
44. Baccarelli A, Martinelli I, Zanobetti A, Grillo P, Hou L, Bertazzi PA, Mannucci PM, Schwartz J. Exposure to particulate air pollution and risk of deep vein thrombosis. Arch Intern Med 2008;168: 920–927.
45. Emmerechts J, Alfaro-Moreno E, Vanaudenaerde BM, Nemery B, Hoylaerts MF. Short-term exposure to particulate matter induces arterial but not venous thrombosis in healthy mice. J Thromb Haemost 2010;8:2651–2661.
46. Puett RC, Hart JE, Yanosky JD, Paciorek C, Schwartz J, Suh H, Speizer FE, Laden F. Chronic fine and coarse particulate exposure, mortality, and coronary heart disease in the nurses' health study. Environ Health Perspect 2009;117:1702–1706.
47. Simkhovich BZ, Kleinman MT, Kloner RA. Particulate air pollution and coronary heart disease. Curr Opin Cardiol 2009;24:604–609.
48. Yang P, Lu C, Hua N, Du Y. Titanium dioxide nanoparticles co-doped with Fe^{3+} and Eu^{3+} ions for photocatalysis. Mater Lett 2002;57:794–801.
49. National Institutes of Health (NIH).Guide for the Care and Use of Laboratory Animals.Washington, DC:National Academy Press; 1996.
50. Oliveira CP, Lopasso FP, Laurindo FR, Leitao RM, Laudanna AA. Protection against liver ischemia-reperfusion injury in rats by silymarin or verapamil. Transplant Proc 2001;33:3010–3014.
51. Nourooz-Zadeh J, Tajaddini-Sarmadi J, Wolff SP. Measurement of plasma hydroperoxide concentrations by the ferrous oxidation-xylenol orange assay in conjunction with triphenylphosphine. Anal Biochem 1994;220:403–409.
52. Buege JA, Aust SD. Microsomal lipid peroxidation. Method Enzymol 1978;52:302–310.
53. Fagan JM, Bogdan GS, Sohar I. Quantitation of oxidative damage to tissue proteins. Int J Biochem Cell Biol 1999;31:751–757.
54. Beauchamp C, Fridovich I. Superoxide dismutase: Improved assays and assay applicable to acrylamide gels. Anal Biochem 1971;44:276–286.
55. Claiborne A. Catalase activity. In: Greenwaid RA, editor. Handbook of Methods for Oxygen Free Radical Research.Boca Raton, FL:CRC Press;1985.
56. Lundquist I, Josefsson JO. Sensitive method for determination of peroxidase activity in tissue by means of coupled oxidation reaction. Anal Biochem 1971;41:567–577.
57. Habig WH, Jakoby WB. Assay for differentiation of glutathione-S-transferases. Method Enzymol 1981;77:398–405.
58. Moron MS, Depierre JW, Mannervik B. Levels of glutathione, glutathione and reductase, glutathione *S*-transferase activities in rat lung and liver. Biochim Biophys Acta 1979;582:67–76.
59. Hissin PJ, Hilf RA. Fluorometric method for determination of oxidized and reduced glutathione in tissues. Anal Biochem 1976;74: 214–226.
60. Jacques-Silva MC, Nogueira CW, Broch LC, Flores EM, Rocha JBT. Diphenyl diselenide and ascorbic changes deposition of selenium and ascorbic in liver and brain of mice. Pharmacol Toxicol 2001;88:119–125.
61. Yee AT. Assay of thiols and disulfides in intestinal lymph. Method Enzymol 1975;251:221–228.
62. Lowry OH, Rosebrough NJ, Farr AL, Randall RJ. Protein measurement with the folin phenol reagent. J Biol Chem 1951;193: 265–275.
63. Stadtman ER, Levine RL. Free radical-mediated oxidation of free amino acids and amino acid residues in proteins. Amino Acids 2003;25:207–218.
64. Chevion M, Berenshtein E, Stadtman ER. Human studies related to protein oxidation: Protein carbonyl content as a marker of damage. Free Radic Res 2000;33:S99–S108.
65. Kasai H, Nishimura S. Hydroxylation of guanine in nucleosides and DNA at the C-8 position by heated glucose and oxygen radical-forming agents. Environ Health Perspect 1986;67:111–116.
66. Evans MD, Dizdaroglu M, Cooke MS. Oxidative DNA damage and disease: Induction, repair and significance. Mutat Res 2004;567: 1–6.
67. Grollman AP, Moriya M. Mutagenesis by 8-oxoguanine: An enemy within. Trends Genet 1993;9:246–249.
68. Pilger A, Rüdiger HW. 8-Hydroxy-2′-deoxyguanosine as a marker of oxidative DNA damage related to occupational and environmental exposures. Int Arch Occup Environ Health 2006;80:1–15.
69. Fortunato JJ, Feier G, Vitali AM, Petronilho FC, Dal-Pizzol F, Quevedo J. Malathion-induced oxidative stress in rat brain regions. Neurochem Res 2006;31:671–678.
70. Lukaszewicz-Hussain A. Activities of brain antioxidant enzymes, lipid and protein peroxidation. Cent Eur J Med 2011;6:588–594.
71. Scandalias G. Response of plant antioxidant defence genes to environmental stress. Adv Genet 1990;28:1–41.
72. Asada K. The water-water cycle in chloroplasts: Scavenging of active oxygens and dissipation of excess photons. Annu Rev Plant Physiol Plant Mol Biol 1999;50:601–639.
73. Crawford NM, Kahn ML, Leustek T, Long SR. Nitrogen and sulfur. In: Buchanan BB, Gruissem W, Jones RL, editors. Biochemistry and Molecular Biology of Plants. Rockville: ASPP, 2000; p 786–849.
74. Sivori JL, Casabe N, Zerba EN, Wood EJ. Induction of glutathione S-transferase activity in Tria-tomainfestans. Mem Inst Oswaldo Cruz 1997;92:797–802.
75. Armstrong JS, Steinauer KK, Hornung B, Irish JM, Lecane P, Birrell GW, Peehl DM, Knox SJ. Role of glutathione depletion and reactive oxygen species generation in apoptotic signaling in a human B lymphoma cell line. Cell Death Differ 2002;9:252–263.
76. Smirnoff N.Antioxidants and Reactive Oxygen Species in Plants.Oxford:Blackwell Publishing;2005.
77. Jovanovic-Galovic A, Blagojevic DP, Grubor-Lajsic G, Worland R, Spasic MB. Role of antioxidant defense during different stages of preadult life cycle in European corn borer (Ostrinia nubilalis, Hubn.): Diapause and metamorphosis. Arch Insect Biochem Physiol 2004;55:79–89.
78. Morrison JP, Coleman MC, Aunan ES, Walsh SA, Spitz DR, Kregel KC. Thiol supplementation in aged animals alters antioxidant enzyme activity after heat stress. J Appl Physiol 2005;99: 2271–2277.
79. Gilbert HF. Thiol/disulfide exchange equilibria and disulfide bond stability. Method Enzymol 1995;251:8–28.